DETECTION OF CLOUD EFFECTS IN MIPAS OBSERVATIONS AND IMPLEMENTATION IN THE OPERATIONAL PROCESSOR

PO-TN-ULE-GS-0002

John J. Remedios [(1)], Reinhold Spang [(1)] and Marco Ridolfi [(2)]

[(1)] *EOS, Space Research Centre, University of Leicester, U.K, email: j.j.remedios@le.ac.uk, r.spang@le.ac.uk.*
[(2)] *Dipartimento di Chimica Fisica ed Inorganica – Università di Bologna, Bologna, Italy, email: ridolfi@fci.unibo.it*

SUMMARY

The Michelson Interferometer for Passive Atmospheric Sounding (MIPAS) instrument measures the intensity of atmospheric radiation emitted in the infra-red spectral region at high spectral resolution in five bands ranging from 685 cm^{-1} to 2410 cm^{-1}. Clouds affect the appearance of the measured spectra at all wavelengths which are sensitive to emission from the layer of atmosphere containing the cloud. Both low resolution (cloud continuum) and high resolution features (complicated spectral lineshapes) can be observed due to the MIPAS resolution of 0.025 cm^{-1} (unapodized). This has two implications. Firstly, spectra containing clouds can affect the quality of the operational trace gas retrievals. Therefore clouds must be identified and flagged prior to retrievals of trace gas concentrations at level 2; thin clouds may be allowed if the retrieval accuracy/stability for trace gases remains good. Secondly, the cloud information constitutes a valuable product in itself. In this report, the development and verification of a successful MIPAS cloud detection scheme is reported. Retrieval simulations and analysis of the MIPAS level 2 data are examined to demonstrate the effects of the clouds and the quality of the data given cloud flagging. The results are excellent and the cloud detection method will be included in the next update of the MIPAS operational processor. The results presented also support the quality of the MIPAS reference atmospheres which are available for use by other instrument teams.

CONTENTS

1 INTRODUCTION

The Michelson Interferometer for Passive Atmospheric Sounding (MIPAS) on ENVISAT is an infra-red Fourier transform spectrometer which observes radiation emerging from the Earth's limb. Vertical profiles of the radiance are obtained by scanning the limb between 6 and 68 km at a spacing of 3 km in the lower atmosphere. Five channels are employed covering a complete wavenumber region between 685 cm^{-1} (14.60 µm) and 2410 cm^{-1} (4.15 µm) at "high" resolution (nominally 0.035 cm^{-1} apodised). In the current operational processor, seven products (temperature and trace gases) are obtained by inversion of the radiance signal to product profiles. This processor includes only limb spectra at the tangent altitudes above 12 km although it has now been shown that useful information exists from 6 km upwards (Carli *et al*., 2002 [1]) and this may be included in future updates. In fact, a large number of additional products are possible from MIPAS throughout the scanned height range including information on many trace gases, aerosol/cloud particles and potentially winds. It is the purpose of this report to describe cloud effects in MIPAS data and their detection.

Clouds absorb, emit and potentially scatter radiation over a broad range of wavelengths in the infra-red. Present in the atmosphere as conglomerates of particles, at least as defined in this study, they include most notably cirrus clouds in the upper troposphere and polar stratospheric clouds in the cold winter stratosphere. The clouds can have profound influences on infra-red spectra of the atmosphere, a sensitivity which is heightened for MIPAS by the use of a limb sounding with its long pathlengths near the tangent point.

Historically, evidence for the infra-red detection of clouds in limb views has been obtained primarily from observations by radiometers integrating the infra-red spectrum over passbands of typically 10 to 100 cm^{-1}. For example, data from the Upper Atmosphere Research Satellite demonstrated the influence of layers of sub-visible cirrus through statistical/seasonal analyses by Mergenthaler *et al*. [2] and Massie *et al*. [3]. Such clouds were shown to exist at upper tropospheric altitudes with occurrence frequencies of up to 40% in the tropics. Polar stratospheric clouds were also observed by the same instruments on UARS and a number of studies, e.g. Taylor *et al*. [4] and Hervig *et al* [5] inferred aspects of the distribution and characteristics of PSCs in both the Arctic and Antarctic.

Two aspects were very clear from these limb sounding studies: 1) the vertical resolution and geometry of limb sounding provided a unique view of very important, high altitude clouds (above 6 km) with small particle sizes (probably less than 20 µm mean radius); 2) the identification of clouds and subsequent flagging (cloud clearing) were central to good retrievals of trace gas profiles from infra-red instruments. It became clear, pre-launch, that although MIPAS is a spectrometer which allows mitigation of some of the cloud effects on trace gas retrievals, it would be necessary to develop a cloud detection method so as to avoid errors in the operational products. The importance of this cloud flagging is shown in this report and a method developed for flagging cloudy data in the MIPAS operational processor. This flagging must be performed for each spectrum (or "sweep") so that the retrieval scheme for trace gases does not ingest cloudy data.

Finally, it is important to realise that the MIPAS data could allow trace gas concentrations to be retrieved in the presence of "thin" clouds. Ideally the MIPAS cloud detection scheme should allow flexible tuning of thresholds to allow retrieval of the maximum amount of trace gas data; for the scientific user community good trace gas data in the presence of clouds would be of great interest. The approach in this study has been to develop such a scheme but to set the thresholds in a quasi-conservative manner such that the cloud processor would reject, for the purposes of trace gas retrieval, all but the weakest cloudy radiances. Pre-launch, settings were derived mainly from studies of the CRISTA instrument (next section).

2 CLOUD DETECTION METHOD

Development of a cloud detection method for MIPAS, pre-launch, was able to draw heavily on experience obtained by the authors in working with data from the CRyogenic Infrared Spectrometer and Telescopes for the Atmospheres (CRISTA) experiment (Offermann *et al*. [6]). The CRISTA experiment obtained low resolution spectra (2 cm^{-1}) data between 710 and 2400 cm^{-1} during two short missions of the CRyogenic Infrared Spectrometer and Telescopes for the Atmospheres (CRISTA); observations were made in November 1994 and August 1997.

The CRISTA experiment provided for the first time, excellent emission spectra of clouds albeit at 2 cm^{-1} resolution. In particular, in the second CRISTA mission, an enhanced altitude grid and latitudinal coverage provided observations of tropospheric (>8 km) and polar stratospheric clouds (PSCs). Tremendous intensity changes could be observed, when the instrument looked into a cloudy region (Figure 1). The enhanced radiation effected the most significant changes in the spectral shape in the wavenumber regions 800 to 950 cm^{-1} and 1150 to 1250 cm^{-1} where parts of the spectrum act as atmospheric windows for cloud/aerosol detection (similarly to surface sensing). Furthermore, it was found that tropical and polar clouds produced very similar changes in the shape of the spectra. Therefore a cloud detection scheme by means of changes in the spectra can work in a similar manner both in the upper troposphere/lower stratosphere (UT/LS) region and in the polar stratosphere.

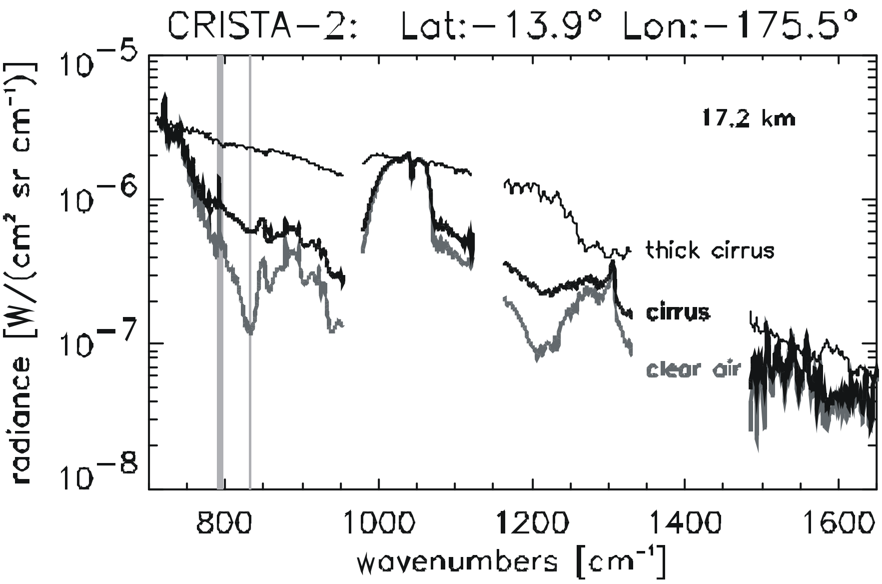

Figure 1: CRISTA spectra of optically thick and thin cirrus clouds as well cloud-free conditions in the tropical region at around 17 km tangent height measured in August 1997. The lines mark the locations of the CI-A mesowindow pairs.

Four important points have arisen from a number of studies of CRISTA data carried out by the authors of this report:

1) It has been shown that clouds can be detected and cloud height estimated using a spectral ratio test;
2) A characteristic spectral signature to PSCs at 820 cm^{-1} has been identified as arising from the presence of HNO_3 dissolved as the nitrate ion (Spang and Remedios, 2003[12]);
3) A combination of 1) and 2) have been used to differentiate sub-visible cirrus, ice PSCs and HNO_3-dominated PSCs;
4) Retrievals of trace gases have been performed for weak cloud (limb optical thickness less than ~0.2 in the infra-red). These aspects are all highly relevant to MIPAS which in addition has the advantage of high spectral resolution enabling better retrieval of trace gases in the presence of optically thin clouds.

In order to build a cloud detection algorithm for MIPAS that was robust, it was decided to develop a cloud detection method that could be verified using the CRISTA data. The method employed is that demonstrated for CRISTA by Spang *et al.* [7] namely the ratio of the integrated radiances in two "mesowindows" which each react differently to the presence of clouds. This simple and robust method was first implemented for CRISTA for a pair of mesowindows, 788–796 cm^{-1} (MW1) and 832–834 cm^{-1} (MW2). The former spectral region is dominated by CO_2 and the latter contains only weak emissions of ozone and CFC11 in comparison to the background aerosol and the enhanced cloud emissions.

In the following the defined ratio will be referred to as the standard CRISTA Cloud-Index (CI-CR) and is given by the following equation:

$$CI\text{-}CR = MEAN\,(\mathrm{MW}_1)\ /\ MEAN(\mathrm{MW}_2) \qquad \textbf{(1)}$$

where *MEAN* stands for the mean radiance value in the specified mesowindows. In this case, MW1/MW2 is such that the cloud index (CI) is large for cloud free conditions (CI>4.5), close to one for optically thick conditions (spectra similar to a black body) and in-between for the transition region from optically thin to optically thick.
Typical values for CI are shown in Figure 2 under conditions with no clouds (dashed curve) and with clouds (PSCs; solid line) in the instrument field-of-view (FOV). The radiance ratio decreases rapidly from one altitude step to the next. Constant values of CI-CR ~1 indicates optical thick conditions. Sensitivity studies for CI-CR with the CRISTA forward radiance model [10] were carried out and reported in [7] and [12]. The analyses show that in the height regime 12-40 km a ratio of CI-CR~2 or smaller can only be produced by a radiation background anomalously enhanced by aerosols or clouds. The temperature dependence of CI-CR is especially weak (<1%/K in the 10-30 km range).

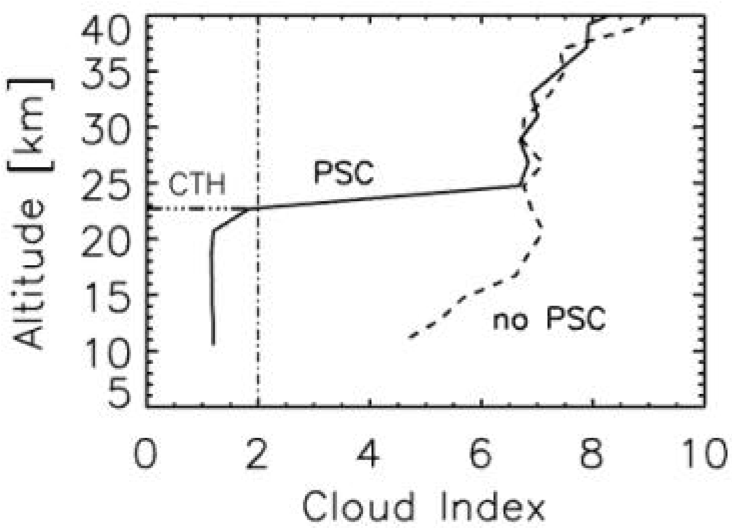

Figure 2: CRISTA cloud index profile [5] for clear sky and cloudy conditions (PSC). A threshold value of 2 - used for the CRISTA analyses - as well the cloud top height (CTH) are indicated by the dash-dotted lines.

Definition of a threshold value for CI also enables a "cloud top height" to be allocated. This corresponds to the top height at which the signature of a cloud is observed within a single CRISTA or MIPAS limb scan. On a statistical basis and within the MIPAS vertical resolution, the cloud top height will most likely be equivalent to the real cloud top height. However individual clouds may be located at higher altitudes than this "observed cloud top height" since the cloud can be located at any point along the line-of-sight of the instrument. This distinction is not important for the requirements of "cloud flagging" but would be more important for the production of cloud products.

3 DEFINITION OF CLOUD MESOWINDOWS FOR MIPAS

The spectral interval originally employed for CRISTA falls in MIPAS band A (cloud index denoted by CI-A). It is desirable to have a cloud flag per spectral channel of MIPAS for two reasons: 1) there may be an invalid spectrum in channel A whilst the other channels (AB, B, C and D) contain valid spectra; 2) different cloud indices may have different sensitivities to cloud effects. Candidate mesowindow pairs were therefore identified by forward modelling of the spectra using a state of the art line-by-line radiative transfer code, the Oxford Reference Forward Model or RFM (Dudhia [8]); reference atmosphere profiles were taken from MIPAS reference atmospheres developed using the methodology of Remedios [9] and spectral data from the HITRAN 1996 database. These mesowindow pairs were then tested on CRISTA data to ensure good statistics. Suitable mesowindow pairs were found in channels B and D (CI-B and CI-D) respectively. Density of spectral lines and variability of the cloud index with altitude prevented similar pairs of mesowindows being defined in channels AB and C. Current threshold values and altitude ranges for use of each ratio are shown in Table 1.

Table 1: Cloud detection settings for MIPAS

Cloud Index MIPAS Band	MW1 (cm^{-1})	MW2 (cm^{-1})	Cloud Index threshold value	Pre-flight MIPAS altitude range (km)	Preliminary MIPAS in-flight altitude range (km)
CI-A	788.20 – 796.25	832.3 – 834.4	1.8	8-60	10*-45
CI-B	1246.3 – 1249.1	1232.3 – 1234.4	1.2	8-50	10*-40
CI-D	1929.0 – 1935.0	1973.0 – 1983.0	1.8	8-32	12*-30

* The height range will be extendable to lower altitudes for mid and high latitudes.

In the ideal case, all three cloud indices would detect the same clouds. However, absorption and scattering characteristics of clouds depend on wavelength. Therefore, differences between the indices might be expected on the basis of the wavelength dependence of the cloud refractive indices or because of differing sensitivities to clouds in the designated mesowindows. This was tested using the CRISTA data.

Figure 3 and Figure 4 shows a comparison of cloud top heights detected using the standard index (CI-CR or CI-A) and the equivalent index for MIPAS band B (CI-B). It is clear that both methods result in a very similar distribution of cloud top heights. The comparison is extended more quantitatively in Figure 5 and Figure 6 which show scatter plots of the cloud top heights determined using CI-A, CI-B and CI-D. Due to the CRISTA altitude grid of around 2 km, any cloud detected by one index at higher or lower altitudes than the 1 to 1 line appears shifted by +/- 2 km, or multiples of 2 km. In the UT/LS region, all three cloud indices agree very well. For example, the CI-B cloud index detects 3.6 % more cloud events than CI-A at higher altitudes and 7.7 % more cloud events at lower altitudes. In total, the CI-B index detects 7.7 % more clouds, mostly due to differences at altitudes mainly below 8 km. The comparison for CI-D shows more events at lower and high altitudes with some scatter. Therefore, pre-flight priority for cloud detection was CI-A, CI-B, and then CI-D.

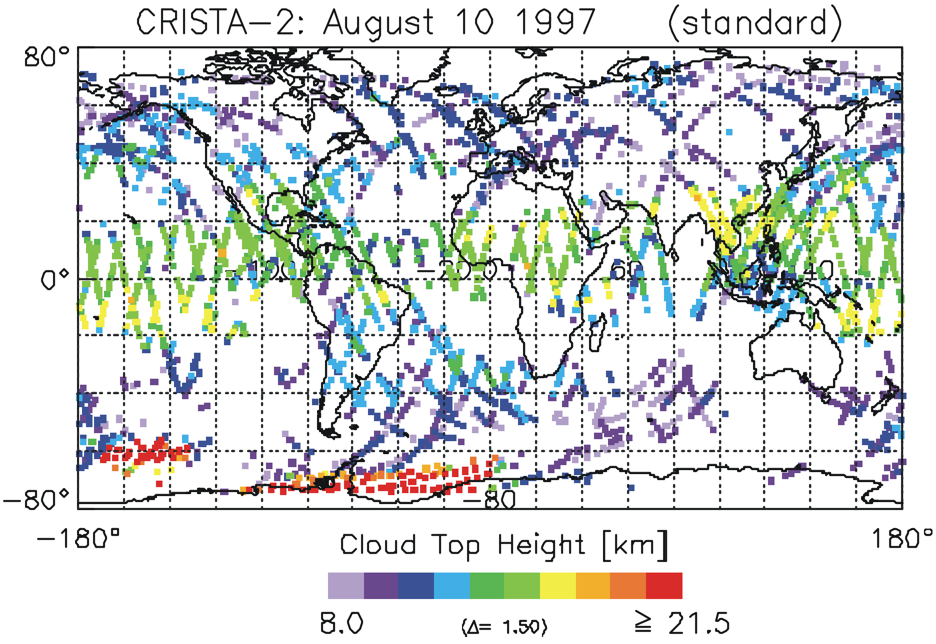

Figure 3: Cloud top height (CTH) computed from CRISTA data using the standard CRISTA index, CI-CR, which is the same as the MIPAS CI-A index. Only the left and right viewing directions of CRISTA were used because the detector of the central spectrometer for the wavelength region equivalent to MIPAS cloud index CI-B had problems in its calibration. Data are for August 10th 1997.

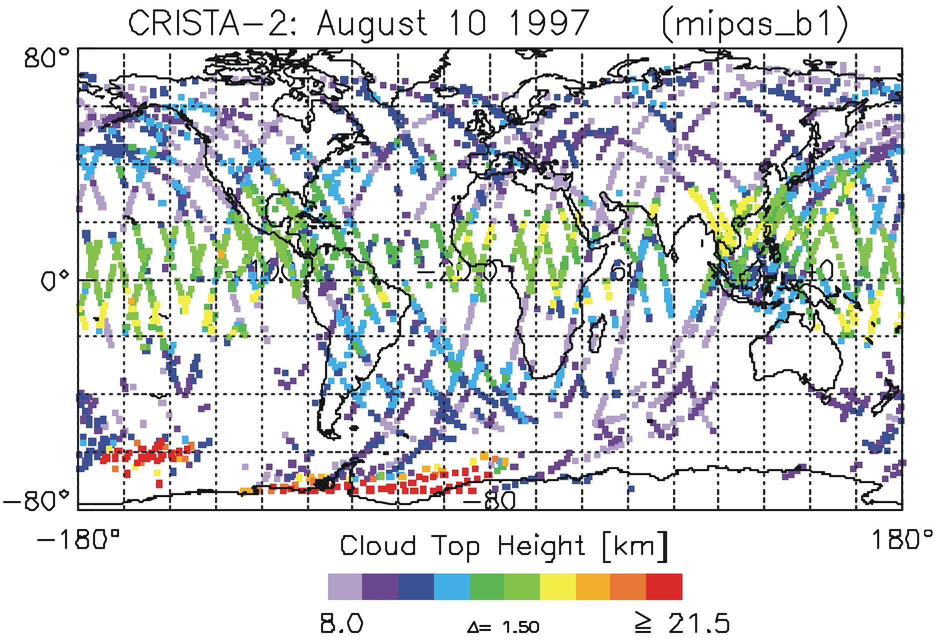

Figure 4: Cloud top height (CTH) computed from CRISTA data using the MIPAS CI-B index. Only the left and right viewing directions of CRISTA were used because the detector of the central spectrometer for the wavelength region equivalent to MIPAS cloud index CI-B had problems in its calibration. Data are for August 10th 1997. The comparison with the standard index (CI-CR, CI-A) in Figure 3 is excellent.

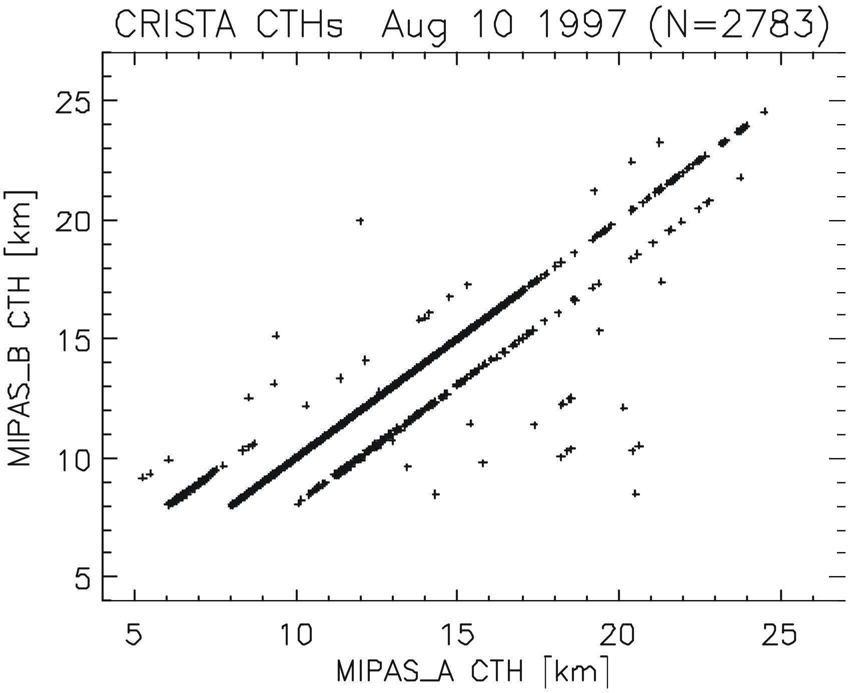

Figure 5: A comparison of cloud top height (CTH) computed from CRISTA data using the CI-A (MIPAS band A) and CI-B (MIPAS band B) indices. The data are for the left and right viewing directions of CRISTA on August 10th 1997.

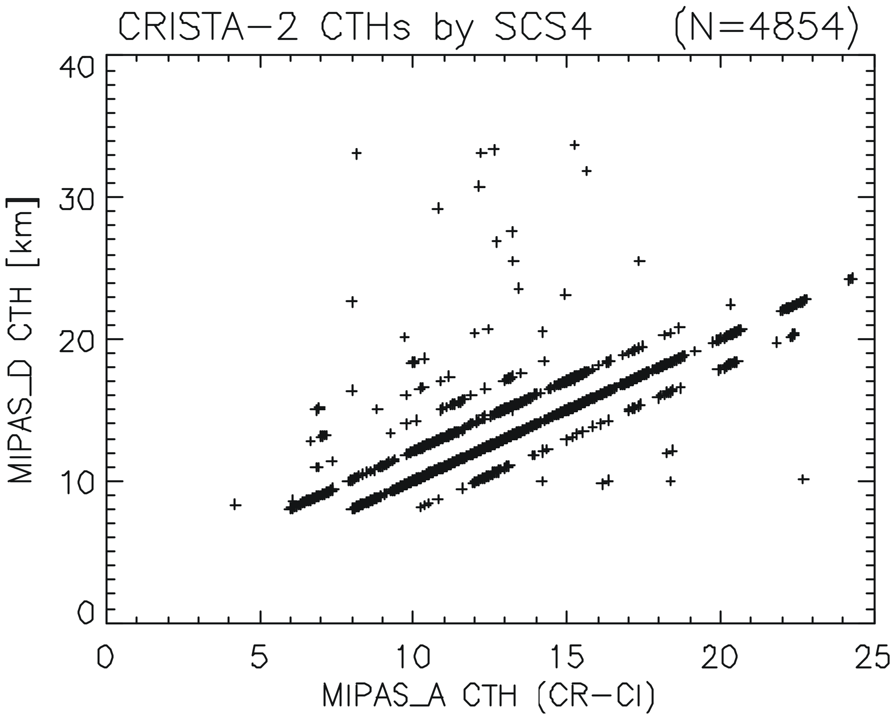

Figure 6: A comparison of cloud top height (CTH) computed from CRISTA data using the CI-A (MIPAS band A) and CI-D (MIPAS band D) indices. The data are for the left and right viewing directions of CRISTA on August 10th 1997.

4 OBSERVATIONS OF CLOUDS IN REAL MIPAS LEVEL 1B DATA

Two sets of MIPAS observations were initially available for analysis, and these immediately provided complementary pieces of information since the first was recorded in April 2002 and the second in July 2002. The April data consist of one orbit of data (orbit 504) containing measurements between 07:26:47.54 and 07:26:47.54 UTC on April 5th 2002. At this time of the year, clouds are expected only in the troposphere and in the region of the tropopause; the tropopause has a mean height of ~17 km at the equator and 9 km at the poles. The July data consist of three contiguous orbits on July 24th 2002 (orbits 2081 to 2083) commencing at 11:21:32.21 UTC until 16:12:04.46 UTC. In contrast to the April time period, the pattern of clouds is expected to be more complicated in the winter pole region (the Antarctic) where the cold temperatures of the stratospheric vortex result in "high" altitude polar stratospheric clouds (PSCs). Such clouds might extended to altitudes of at least 25 km and appear differently in MIPAS spectra due to their differing composition and mean size relative to tropospheric clouds; PSCs are nitric acid hydrates potentially in co-solutions with sulphuric acid and water ice crystals.

The observation of cloud spectra in MIPAS constitutes a first order validation test for the level 1b spectra derived from the instrument's "raw mode" data, and the confirmation of the expected spectral characteristics of clouds. The latter is important for the implementation of the cloud detection method in the prototype pre-level-2 processor. The orbits of data have therefore been carefully examined for cloud effects and examples are shown in Figure 7 to Figure 9.

Figure 7 and Figure 8 show spectra of a tropical cirrus cloud at an altitude of 13.5 and 16.5 km respectively, both in orbit 504 and only 4 minutes apart. If the instrument is looking into a cloudy region of the atmosphere one can observe an obvious offset in the spectra, for example of around 1-2 mW / cm^2 sr cm^{-1} in the MIPAS band A spectral range. Optically very thin cloud may produce significantly smaller continuum offsets. The spectrum in Figure 7 shows very pronounced all expected spectral features of a non-cloudy spectrum, for example the very broad CFC11 emissions between 835 and 855 cm^{-1}. In this case, accurate trace gas retrievals might be still possible. In contrast the spectrum in Figure 8 is strongly disturbed by the cloud emissions. Parts of the spectrum are similar to the emission of a black or grey body. In addition, absorption features are easy to detect in the spectra, especially for wavenumbers greater than 750 cm^{-1}. These features are caused by scattering effects, whereby light coming from the lower troposphere and/or the ground is scattered by the cloud into the line of sight of the instrument. Spectra like this will produce a lot of difficulties for the level 2 retrieval.

Figure 9 shows a spectrum at 16.5 km altitude of a PSC event in the Antarctic. Obviously the spectrum shows an enhanced offset similar but weaker than the two cirrus cloud examples. Large parts are again very similar to a black/grey body emission. No absorption signatures are found in this example, which could be due to lower optical thickness of the cloud (lower offset).

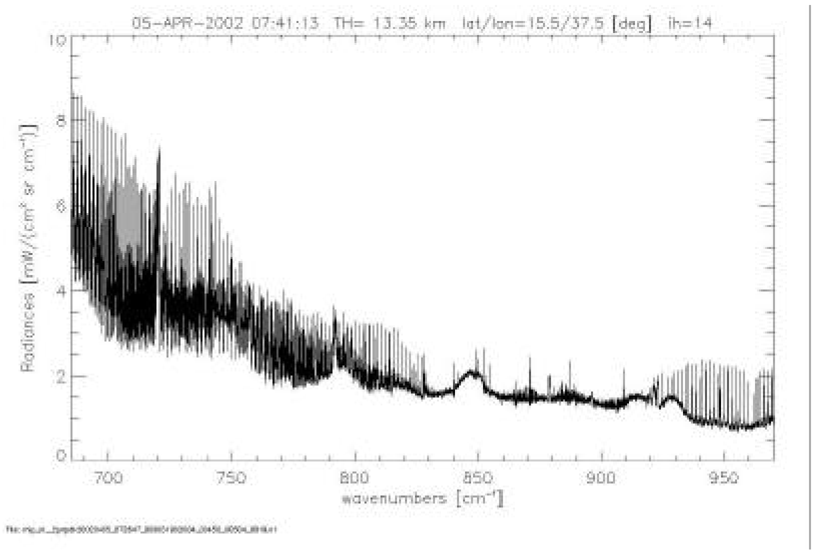

Figure 7: MIPAS spectrum of orbit 504 of an optically thin cirrus cloud in the equatorial region. Radiance units in microW/cm^2 sr cm^{-1}.

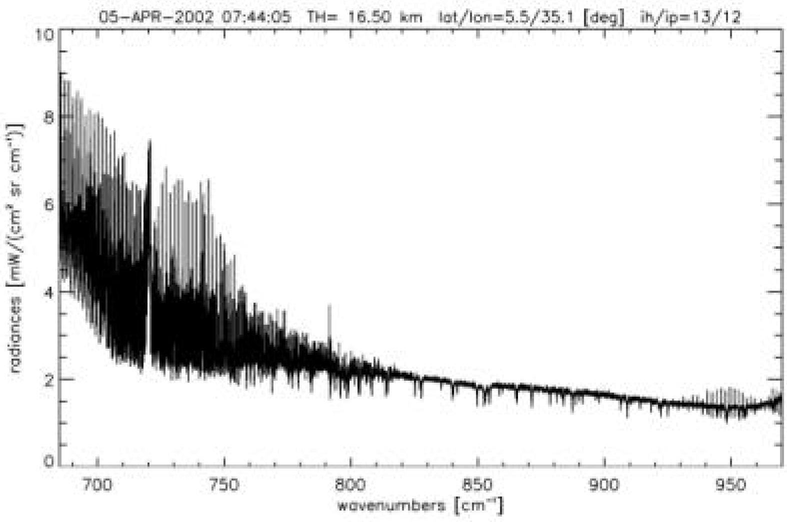

Figure 8: MIPAS spectrum of orbit 504 of an optically thick cirrus cloud including absorption features in the equatorial region (16.5 km tangent height). Radiance units in micro W/cm^2 sr cm^{-1}.

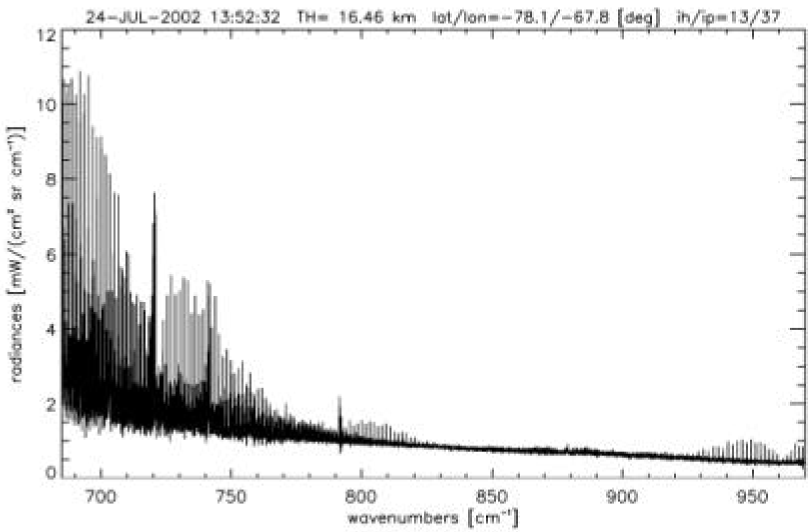

Figure 9: MIPAS band A spectrum in orbit 2082 of an optically thick polar stratospheric cloud at 16.5 km height. Radiance units in micro W/cm^2 sr cm^{-1}.

Figure 10 presents one of the first observed spectra of PSCs from MIPAS recorded in the Antarctic vortex at a tangent altitude of 19.5 km. Again, the obvious effect of the PSC cloud can be distinguished as the broad scale continuous offset (*cloud continuum*) as opposed to the sharp spectral lines which are due to atmospheric gases. Variations in the large scale spectral dependence are the potential source of information on PSC composition as noted previously. The expanded view in Figure 10(b) amplifies a point made previously for the cirrus clouds, namely the scattering of tropospheric radiation into the limb path. Here we illustrate the complicated shape of the observed spectral *lines* where the wider pressure-broadened absorption shape to some lines results from tropospheric gas contributions whereas the sharp emission lines are a result of stratospheric contributions. The effect of the scattering is therefore complicated but revealing and depends on the height/location of the cloud along the line-of-sight, the temperature of the cloud and the mean size of the cloud particles. Hence these spectral features can be exploited to deliver mean cloud particle size from infra-red spectral observations.

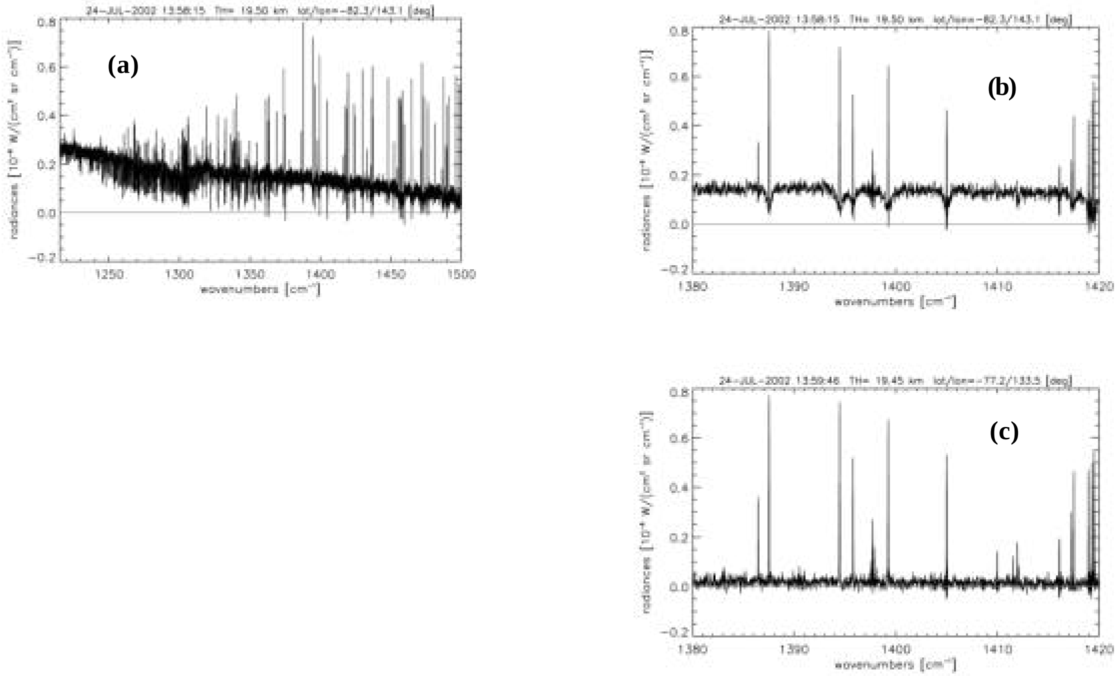

Figure 10: First spectrum of an Antartic vortex PSC observed by the MIPAS on ENVISAT. Data are provided by the ESA and are preliminary but with expected calibration suitable for this purpose. (a) PSC at 19.5 km tangent height as observed in the MIPAS B band; (b) Detailed section of the same PSC spectrum near 1400 cm^{-1}; (c) “Clear sky” spectrum at 19.45 km for a nearby profile. Radiances are in units of ?W/(cm^2 sr cm^{-1}).

The tremendous detail to the spectra strongly encourages the development of cloud products to complement the existing operational trace gas products for MIPAS. A pre-requisite is an investigation of the spectral dependences shown by MIPAS both by direct examination of the data and by forward modelling. This would also enable channels for a future limb cloud imager (LCI) to be specified so as to deliver a much stronger scientific return than previous concepts.

The spectra observed by the MIPAS instrument have already revealed some excellent detailed features of clouds, as anticipated from CRISTA, with features present at high spectral resolution. The chief features of the cloud distribution can be identified, including clouds near the tropopause in the tropical regions and PSCs at higher altitudes in the Antarctic winter. Both optically thin and optically thick clouds have been observed with characteristic spectral features. For thin clouds, the effects of local gas absorption and emission lines are present, potentially allowing co-incident detection of clouds and retrieval of valid gas densities. In contrast, thick clouds show strong offsets at all locations in the spectra and for sufficiently dense clouds, display the effects of the scattering of tropospheric radiation into the limb view from below the cloud. The scattered radiation exhibits high spectral resolution effects, thereby demonstrating the value of the high spectral resolution of MIPAS.

5 VERIFICATION OF THE CLOUD INDEX SETTINGS FOR MIPAS

Verification of the cloud index settings for MIPAS required checks on the cloud detection with the three mesowindow pairs, checks on the altitude range over which the cloud detection scheme could be applied (the in-flight altitude range), and initial checks on the settings for the cloud threshold tests. The last of these primarily requires a check on errors caused in trace gas mixing ratios by cloud effects and is discussed in detail in sections 6 and 7. The first two factors are considered in this section.

The in-flight altitude range was determined from early MIPAS data for approximately 4100 profiles which were available for September 2002 (between the 7th and the 17th). Cloud indices for all three mesowindow pairs were computed off-line. A plot for a composite of September 2002 data is shown in Figure 11, for CI-A, which represents the first global map of cloud top heights from MIPAS data. Very similar plots are obtained for CI-B and CI-D.

The doud index data have also been examined as as vertical profiles (Figure 12) and inter-compared. Excellent agreement was found with a total of 1067 cloud occurrences detected through CI-A, 1158 through CI-B and 1292 through CI-D when the threshold values in Table 1 were applied. Furthermore, 96% of those detected from CI-A in this period were also detected using CI-B and 98% of those detected from CI-B were flagged using CI-D. This implies that either CI-D, for example, is more sensitive to clouds or else the threshold value is set slightly more stringently for CI-D. Below 12 km, forward model calculations show that water vapour can a problem in the tropics and could limit the use of CI-D here; this effect could also be present for the other cloud indices below 10 km. Preliminary investigation suggests that at other latitudes CI-D displays more sensitivity to clouds than the other indices. The low altitude thresholds for all three indices are therefore set somewhat conservatively at this stage and could be extended downwards following further research. At high altitudes, the reduction in the upper altitude threshold from MIPAS to CRISTA is because of the lower signal-to-noise in MIPAS spectra for a single spectrum. Finally, it is worth remarking that CI-D shows a distinct day/night difference due to emission from NO in the atmosphere primarily from the thermosphere.

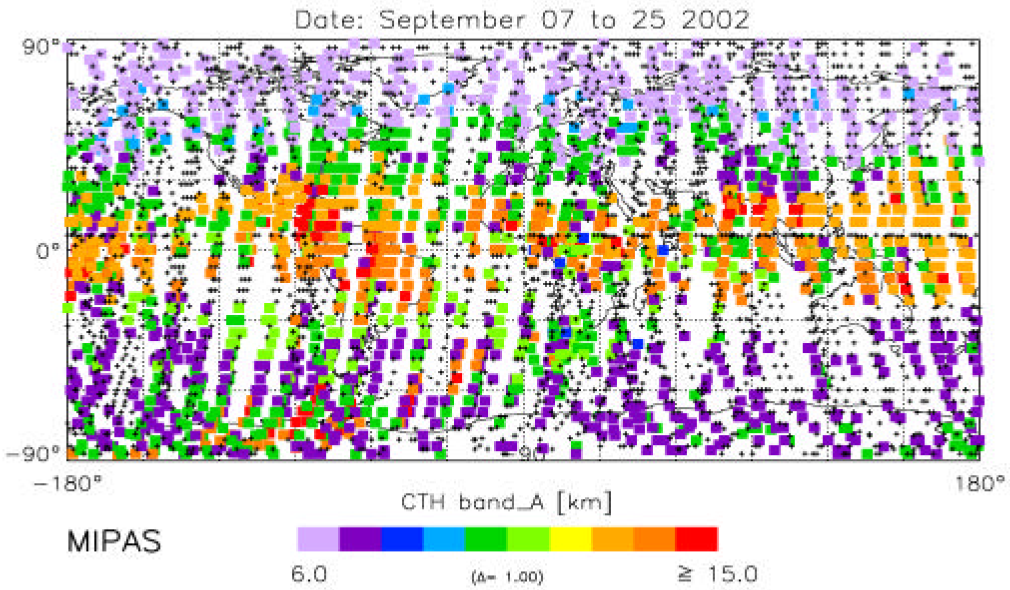

Figure 11: The first global cloud top height map computed from MIPAS level 1b data using CI-A with a threshold of 1.8. The appearance of cirrus clouds in the tropical upper troposphere and polar stratospheric clouds in the Antarctic polar winter can be observed.

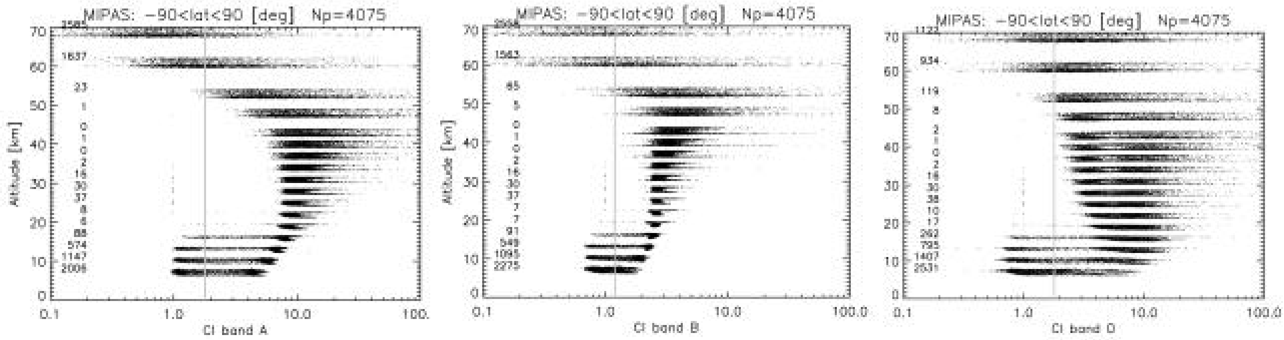

Figure 12: Comparison of the three cloud indices for the MIPAS detector bands A, B, and D. Threshold-values for clouds are indicated by the grey vertical lines. Measurements at all latitudes between September 7 and 17. Numbers for observations below the cloud threshold are superimposed.

6 RETRIEVAL SIMULATIONS FOR TRACE GASES IN THE PRESENCE OF CLOUDS

Since the Level 2 algorithm implemented at launch does not model properly the optical properties of douds (e.g. scattering from particles or droplets is not modeled), exclusion of cloud-contaminated observations from the Level 2 inversion process represents an accuracy improvement of the retrieved profiles. In order to assess the impact of clouds in Level 2 retrievals we analyzed the differences between profiles obtained by alternatively including and excluding from the inversion procedure the cloud-contaminated observations identified by the cloud-detection algorithm described above in section 3.

The Level 1b spectra relating to MIPAS orbit 2081 (acquired on July 24th, 2002) were supplied as input to the so called ML2PP (MIPAS Level 2 Prototype Processor) which, after the initial pre-processing stage, generated input files (observational data, in particular) for the ORM (Optimized Retrieval Model, algorithm representative of the ESA's on-line Level 2 processor). Two sets of ORM input files were generated corresponding to observations selected with and without making use of the cloudy sweeps identified by the cloud-detection algorithm. Starting from these two sets of observations the ORM was run (twice), using the standard set of auxiliary data adopted throughout the whole commissioning phase (Version Jul01) and processing setup parameters optimized on the basis of orbit 2081 data (internal IFAC/UBOL Version 4). The discrepancies between MIPAS key profiles obtained from the two runs were compared with the ESD associated with the profiles themselves. Figure 13 reports, for each retrieved target parameter (indicated on the top of each map), the differences between profiles retrieved in the two runs divided by the related ESD. Values of the plotted ratio greater than one indicate a significant difference between profiles retrieved with and without inclusion of cloudy observations in the retrieval process and therefore a significant systematic error due to clouds. From Figure 13 it is evident that, as expected, for all the target parameters the main differences between retrieved profiles are localized in correspondence to the limb scans containing cloudy sweeps (namely scans 19, 21, 22, 37, 38, 39, 40, 41, 56, 57, 60, 61, 62, 63, 64, 65). The large differences between profiles retrieved in the two approaches however are not localized to the corresponding cloudy sweeps. We rather observe an upward error propagation in the retrieval procedure. Furthermore, since the profiles retrieved at a given scan are used to build the initial guess atmosphere for the subsequent scan, we also observe a mild horizontal propagation of the error induced by the presence of clouds in the observations (possibly this latter effect could be avoided using more stringent convergence criteria).

Beyond the elimination of the systematic errors induced by clouds, excluding cloudy observations from Level 2 analysis leads in general to more stable retrievals, less oscillating profiles and smaller values of the chi-square cost function. This statement is supported by Table 2, in which we report, for all the MIPAS key targets, the average (over analyzed scans) number of iterations required to reach the convergence, the average final chi-square and the average Profile Oscillation Quantifier (POQ) for the two test cases with cloud filtering (CD) and without cloud filtering (noCD).
For an individual scan the POQ is defined as:

$$POQ = 100 \cdot \sqrt{\frac{\sum_{j=2}^{N_{pts}-1}\left[\frac{(x_j - \bar{x}_j)}{(x_j + \bar{x}_j)\cdot 0.5}\right]^2}{N_{pts} - 2}} \tag{1}$$

where x_j is the profile under consideration at altitude z_j, N_{pts} is the number of retrieved profile points and $\bar{x}_j$ is calculated as:

$$\bar{x}_j = x_{j-1} + \frac{x_{j+1} - x_{j-1}}{z_{j+1} - z_{j-1}} \cdot (z_j - z_{j-1}) \tag{2}$$

In practice the POQ represents the percentage r.m.s. distance between each retrieved profile point and the value of the profile (at the same altitude) obtained from interpolation between the two adjacent points. Therefore the POQ quantifies the oscillations of the retrieved profile.

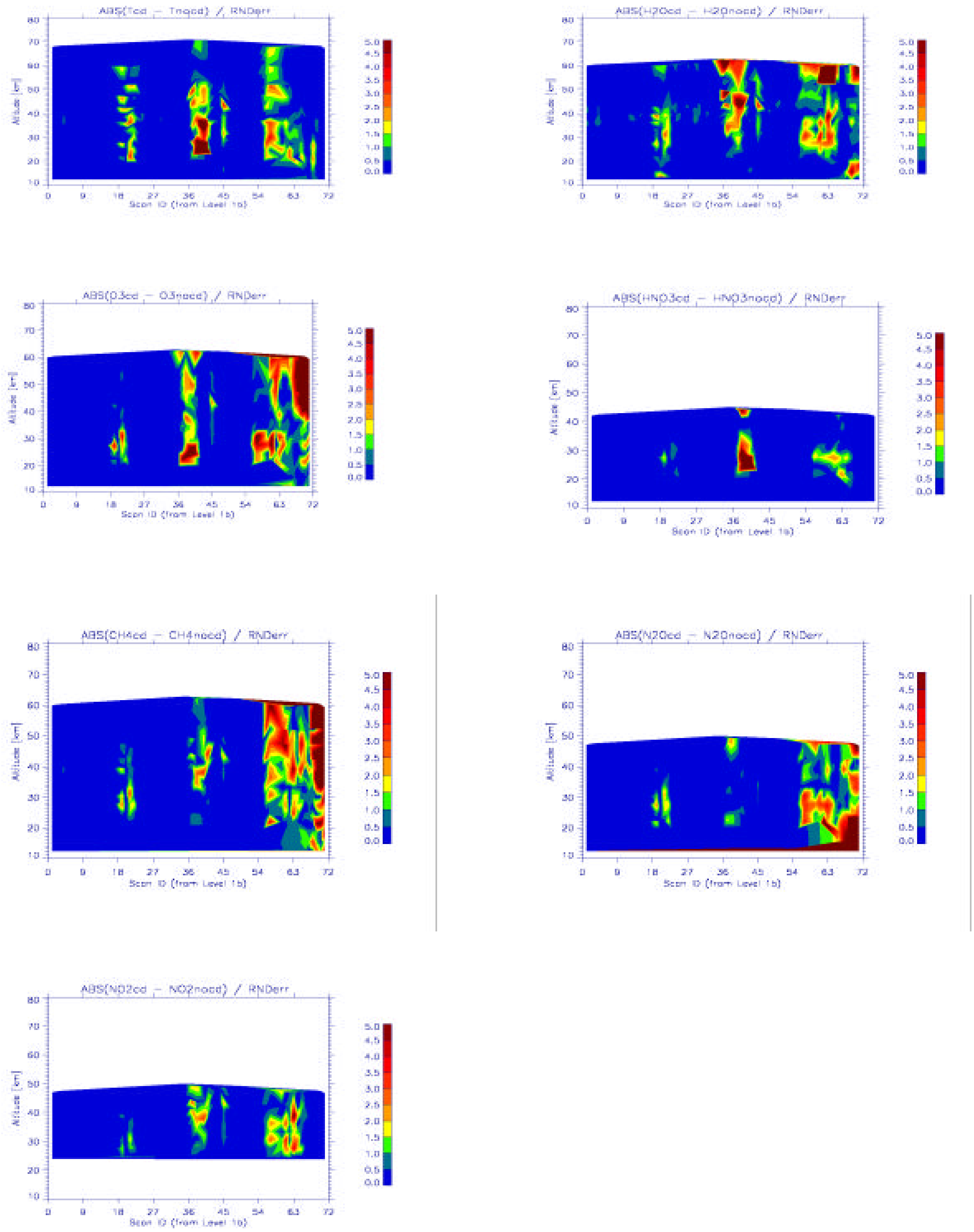

Figure 13: ESD-normalized differences between target parameters (indicated on the top of each map) retrieved with and without inclusion of cloudy observations in the retrieval analysis.

Species	Avg. N. Iterations		Avg. Final CHI2		POQ	
	noCD	**CD**	**noCD**	**CD**	**noCD**	**CD**
pT	2.63	2.21	2.03	1.82	2.13	2.00
H_2O	3.10	1.13	1.42	0.98	30.0	21.3
O_3	2.94	1.27	7.66	1.22	32.8	25.9
HNO_3	2.94	1.46	1.48	1.23	73.7	67.8
CH_4	3.46	1.25	8.17	1.07	33.1	26.3
N_2O	3.04	1.15	5.01	1.05	54.4	41.2
NO_2	1.64	1.67	1.04	1.04	30.6	31.3

Table 2: Average values of number of iterations, final chi-square and Profile Oscillation Quantifier (POQ) for all MIPAS key species, for the considered cases with (CD) and without (noCD) cloud filtering applied.

7 EFFECTS OF CLOUDS ON MIPAS LEVEL 2 TRACE GAS RETRIEVALS

The work described in the previous sections clearly demonstrates the need for cloud effects to be masked in operational level 2 processing. The critical question for the cloud detection and flagging, as far as implementation for the level 2 processor is concerned, is the correct setting of the cloud flag and hence the threshold values for the cloud indices. There are a number of ways to examine cloud effects on derived level two trace gas mixing ratios, for example, scatter plots of retrieved trace gas concentrations versus cloud index value, comparisons of the altitude dependence of trace gas concentrations to means and standard deviations from reference atmospheres, and comparisons of zonal mean cross-sections of retrieved and reference atmospheres. In this report, the altitude dependence of the trace gas retrieved products is examined with respect to the MIPAS standard atmospheres V3.1 (developed using the methodology of Remedios [9]).

Figure 14 to Figure 19 show comparisons between MIPAS data and the MIPAS reference atmospheres for the tropical region (defined as 20ºS to 20ºN) as observed by MIPAS in September 2002. Available data allowed 930 profiles to be included in the analysis which was performed both for the unflagged level 2 data (as currently output by the operational processor) and for level 2 data which were flagged for the effects of clouds. Both the individual points and the average of the MIPAS data are plotted to allow comparison to the mean and variability of the reference atmospheres; variability is represented by maximum/minimum profiles. The reader is cautioned that more detailed comparisons require further account to be taken of the averaging kernels of the retrieval and this is being undertaken in a further study.

The plots in Figure 14 and Figure 15 are for ozone and methane respectively. Above 20 km, it is clear that the average MIPAS ozone and methane data agree very well with the mean reference profile. Retrieved ozone appears to be slightly higher at the peak of the ozone profile by about 10%. In the higher part of the atmosphere, the retrieved ozone decreases at a slightly faster rate than the reference profile. Very encouragingly, the scatter in the MIPAS data compares well with the sigma from the reference atmosphere, particularly for ozone. There is evidence that the scatter in the methane data is higher than the reference variabilities. Below 20 km, cloud effects make a considerable difference to both ozone and methane values. The unflagged level 2 data show values which can be an order of magnitude higher than would be expected from the reference atmosphere. Use of a cloud flag (CI-A<1.8 was employed here) moves the average to much smaller values in closer agreement with the reference state. Here, methane constitutes a better test than ozone for the cloud effects because of our relative lack of knowledge of upper tropospheric ozone values globally. The methane plot suggests that the cloud threshold might not be stringent enough since small deviations are still observed in the flagged methane data near 12 km. As the upper troposphere might be expected to appear relatively well-mixed for methane, this geophysical test provides a good validation for the cloud thresholds.

Similar work has been performed for the other MIPAS operational products (Figure 16 to Figure 19) and the conclusion is the same for all species: (1) the cloud detection scheme is necessary for level 2 retrieved data to be utilised fully; (2) the performance of the reference atmospheres and the non-cloudy MIPAS data is excellent in encapsulating mean profiles and variabilities. The cloud detection scheme and threshold settings outlined here are therefore to be implemented in the MIPAS operational processor.

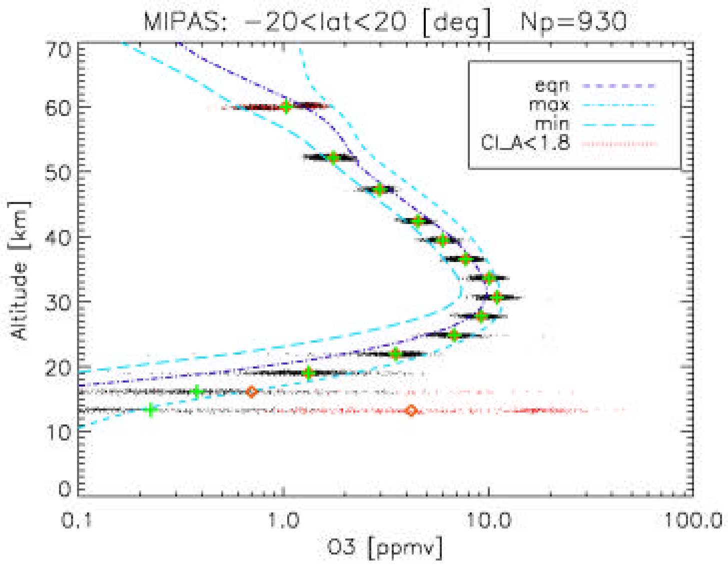

Figure 14: Comparison of the MIPAS tropical data for ozone in September 2002. Black and red dots are the MIPAS retrieved data with diamonds for the mean of the unflagged MIPAS retrievals and crosses for the mean of the cloud-flagged data (see 20 km and below); black=non-cloudy data, red=cloud affected data as detected by the cloud test with CI-A. The tropical reference atmosphere is the dot-dashed line and the dashes are references representing the expected minimum and maximum extremes of the mixing ratio at each altitude.

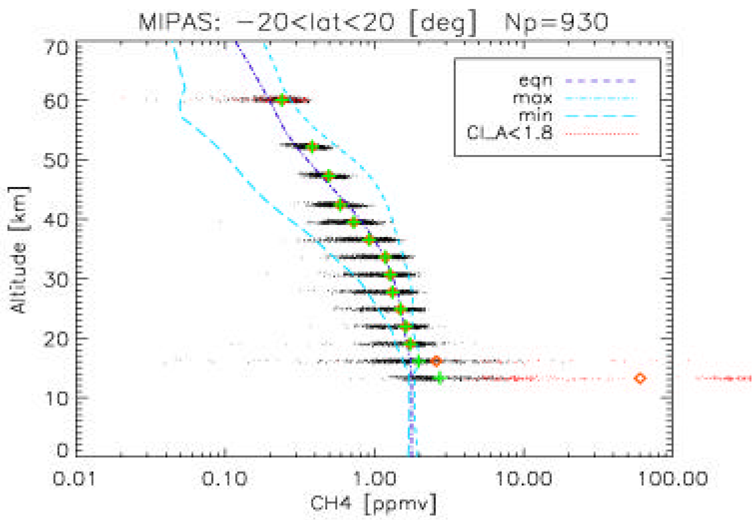

Figure 15: Comparison of the MIPAS tropical data for methane in September 2002. Black and red dots are the MIPAS retrieved data with diamonds for the mean of the unflagged MIPAS retrievals and crosses for the mean of the cloud-flagged data (see 20 km and below); black=non-cloudy data, red=cloud affected data as detected by the cloud test with CI-A. The tropical reference atmosphere is the dot-dashed line and the dashes are references representing the expected minimum and maximum extremes of the mixing ratio at each altitude.

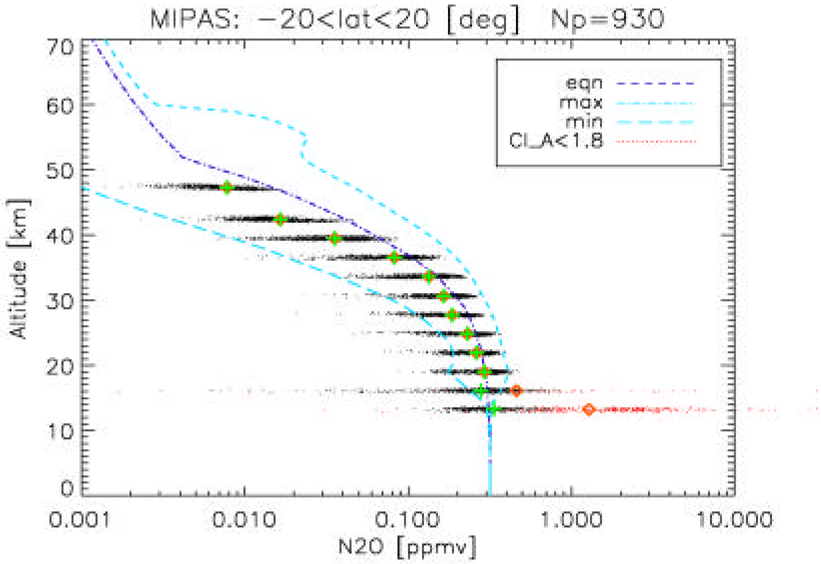

Figure 16: Comparison of the MIPAS tropical data for N_2O in September 2002. Black and red dots are the MIPAS retrieved data with diamonds for the mean of the unflagged MIPAS retrievals and crosses for the mean of the cloud-flagged data (see 20 km and below); black=non-cloudy data, red=cloud affected data as detected by the cloud test with CI-A. The tropical reference atmosphere is the dot-dashed line and the dashes are references representing the expected minimum and maximum extremes of the mixing ratio at each altitude.

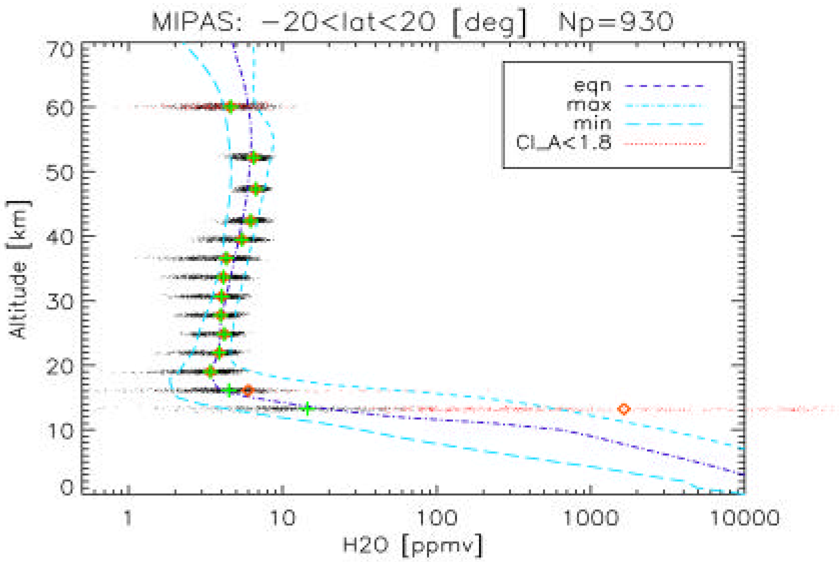

Figure 17: Comparison of the MIPAS tropical data for H_2O in September 2002. Black and red dots are the MIPAS retrieved data with diamonds for the mean of the unflagged MIPAS retrievals and crosses for the mean of the cloud-flagged data (see 20 km and below); black=non-cloudy data, red=cloud affected data as detected by the cloud test with CI-A. The tropical reference atmosphere is the dot-dashed line and the dashes are references representing the expected minimum and maximum extremes of the mixing ratio at each altitude.

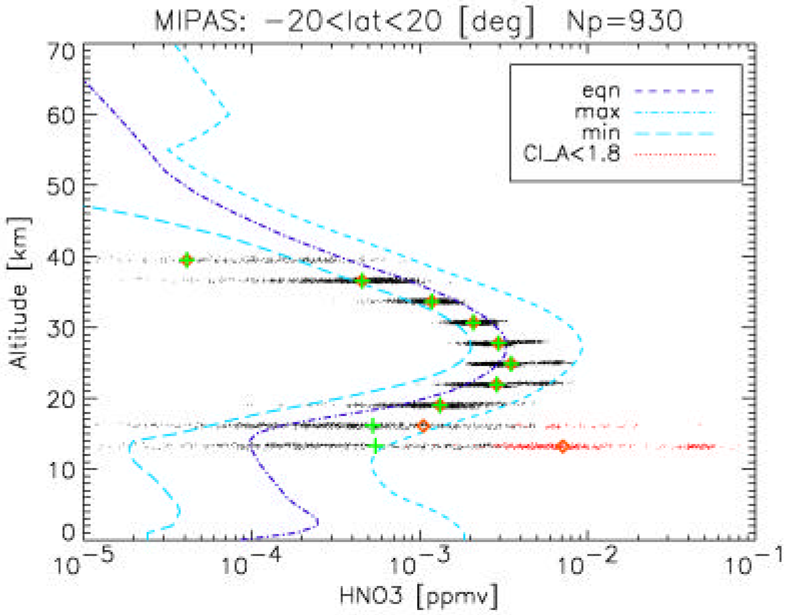

Figure 18: Comparison of the MIPAS tropical data for HNO_3 in September 2002. Black and red dots are the MIPAS retrieved data with diamonds for the mean of the unflagged MIPAS retrievals and crosses for the mean of the cloud-flagged data (see 20 km and below); black=non-cloudy data, red=cloud affected data as detected by the cloud test with CI-A. The tropical reference atmosphere is the dot-dashed line and the dashes are references representing the expected minimum and maximum extremes of the mixing ratio at each altitude.

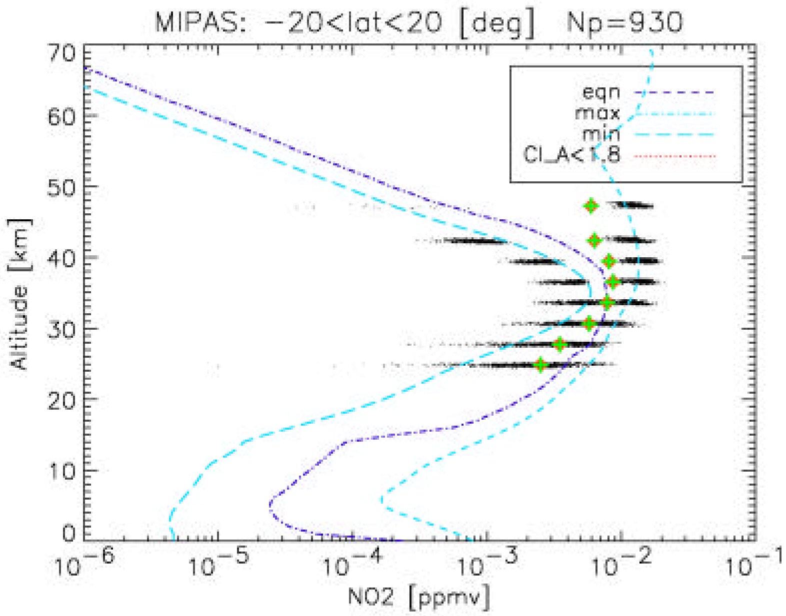

Figure 19: Comparison of the MIPAS tropical data for NO_2 in September 2002. Black and red dots are the MIPAS retrieved data with diamonds for the mean of the unflagged MIPAS retrievals and crosses for the mean of the cloud-flagged data (see 20 km and below); black=non-cloudy data, red=cloud affected data as detected by the cloud test with CI-A. The tropical reference atmosphere is the dot-dashed line and the dashes are references representing the expected minimumand maximum extremes of the mixing ratio at each altitude.

8 SUMMARY AND CURRENT STATUS

A cloud detection scheme has been successfully implemented in the prototype operational processor. This cloud scheme will be effective from 10 km to 45 km and further work should refine the scheme such that altitudes below 10 km can be adequately addressed. The cloud detection scheme has been shown to be necessary to utilise level 2 retrieved data fully. A further consequence of this test has been to demonstrate the excellent agreement in the tropical region between the mean and variabilities of cloud-flagged MIPAS gas concentration data and the corresponding quantities for reference atmospheres. This also demonstrates the quality of the reference atmospheres. Finally, the cloud data are valuable in themselves and should be made available as an additional MIPAS product (s). For example, the use of appropriate radiance ratios could enable maps of polar stratospheric cloud (PSC) types to be obtained. Such information has potential as part of a Global Monitoring for the Environment and Security (GMES) system for atmospheric ozone.

The current status of the cloud detection system can be summarised as follows:

1. A cloud detection scheme has been defined based on the ratio of signals in 2 “mesowindows” (a mesowindow pair). The approach has been validated by using CRISTA data and applying tests based on expected geophysical behaviour.

2. Cloud detection mesowindow pairs have been established in 3 bands: Band A, B, and D. Band A is currently of the highest priority, then Band B and finally Band D.

3. The flagging of clouds is performed via a threshold test. The value of this threshold is currently specified for each mesowindow and is <u>constant</u> for all altitudes, latitudes and time. A software option is already defined in the operational processor for the thresholds to be set as a function of altitude and latitude (IG2 – 4 seasons, 6 latitude bands). However, such values have to be defined if appropriate.

4. The cloud detection and flagging scheme has been shown to give a very significant improvement on the quality and convergence of retrievals of the level 2 trace gas concentrations and on the use of the data for validation/scientific exploitation.

5. The use of a DDS link to the Rutherford Appleton Laboratory has proved to be very useful in the derivation and diagnosis of cloud index profile data on a daily basis.

The cloud flagging scheme will be updated in the operational processor shortly (actually implemented on 23/07/2003). However, no cloud specific information will be output by the processing software (Sven Bartha, Astrium). It will therefore be necessary to implement one of the products outlined in section 10 to capitalise on the new information.

Further work is necessary to fully optimise the cloud detection thresholds, particularly at altitudes below 10 km in the tropics. In addition, the provision of cloud information for the AB and C bands should be examined; cloud flagging in these channels is likely to require information from within microwindows because of the density of lines in the spectra and saturation effects. Since the variability of trace gases, and water vapour in particular is uncertain, the cloud index approach should be validated over a period of 12 months. Long term activities should include consideration of the effects of large injections of volcanic aerosol into the upper troposphere/lower stratosphere, and the effects of any drifts in instrument performance.

Finally, the cloud index detection information for MIPAS will provide valuable information to the Atmospheric Chemistry Validation Team (ACVT) involved in ENVISAT/MIPAS validation. Therefore, cloud index profiles are now being processed in near real-time (NRT) and maps of cloud top height can be found at http://www.leos.le.ac.uk/mapscore.

9 RECOMMENDATIONS FOR FUTURE UPDATES AND VALIDATION SUPPORT

There are a number of areas where the highly successful cloud scheme needs further investigation. This work should be performed over the next two years.

i. Examine and update table of cloud detection threshold values over a complete year of MIPAS data.

The current thresholds need to be examined over a range of geophysical conditions including polar winters (stratospheric louds), polar summers (tropospheric clouds), mid-latitudes (summer/winter changes in water vapour) and tropics (variability in water vapour). The desirability of specifying altitude and latitude dependent threshold values will be identified as part of this work.

ii. Investigate the use of D band cloud MW pair at low altitudes (< 10 km).

The D band mesowindow appears so far to be more sensitive to clouds than other mesowindows, probably because of the shorter wavelengths employed. However, there is also a possible influence of water vapour variability at the lowest altitudes (below 10 km) and a potential uncertainty arising from the dependence of the D band cloud index on day/night. These effects will be investigated.

iii. Investigate the detection of clouds using operational MWs for each target gas.

The approach of defining mesowindows for cloud detection has produced good results for channels A, B and D. However, there are reasons why the definition of clouds from trace gas microwindows might also be desirable. Firstly, it is difficult to find appropriate mesowindows in bands AB and C hence the operational processor does not have full redundancy of cloud MWs in the case of poor spectra in one or more channels. Secondly, the spectral variation of cloud effects and retrieval sensitivity to clouds suggest that there should be a check on the usefulness of a closer tie of cloud flagging to individual trace gas retrievals. For example, it could be that cloud flagging is best performed with an MW in the same band as a particular trace gas retrieval. This effect can be investigated by examining the variations of the continuum retrieved as part of the trace gas retrieval relative to the cloud index derived from the mesowindow approach.

iv. Provision of cloud data for ACVT validation of MIPAS.

Since cloud data flagging is not currently implemented in the operational processor, and since clouds profoundly affect the retrieved data, it is important that expert guidance and cloud flagging data are supplied to the ACVT team. As demonstrated by the University of Leicester results, the use of cloud flagging allows valid comparisons to be made. Therefore, appropriate cloud information should be derived and supplied to the ESL, cal/val and ACVT teams for all data prior to the operational processor update. There is also a requirement for the supply of NRT cloud mapping to the ACVT team for flight planning but this is probably a different issue to algorithm update and verification studies.

v. Long term monitoring and investigation

There are a number of aspects that need further investigation and may prove to be important in future years. Certainly long term monitoring and verification will be required. The aspects identified so far are:

a) ***Volcanic eruptions.*** Both minor and major volcanic eruptions can occur (cf. Mt. Pinatubo effect on UARS data). Effects can be trapped with the cloud detection but the effect of spectral variations (sulphate aerosol) may lead to quite different impacts on individual trace gas retrievals. These will need to be assessed and could lead to quite different microwindow selections resulting from major eruption influences. [A link to the volcanic eruption network should be established, perhaps in the framework of the new Quality Working Group or QWG].

b) ***Instrument changes.*** Current assessment of the MIPAS instrument has indicated that zero offsets are very small. However, this may change in future and could directly affect the cloud index profile determination. The signal-to-noise levels of MIPAS have already been shown to be a problem and further changes in NESR (noise equivalent spectral radiance) should be monitored and related to the thresholds for cloud determination.

c) ***Changes in upper tropospheric concentrations of gases.*** The detection of cirrus clouds is related to assumptions on the likely variability of upper tropospheric gases which are not well understand (and therefore a goal for the MIPAS user community!). This is particularly the case for water vapour. The limits for cloud detection will need to be verified on a long term basis to allow for seasons and interannual variability.

10 RECOMMENDATIONS FOR NEW PRODUCTS

The cloud data constitute valuable new products from ENVISAT and should be implemented as new products arising from the excellent MIPAS observations. Clearly timescales will depend on resources but one can imagine that version 1 of items a) and b) can be specified within the first half of 2003 (following validation), cloud location and cloud composition, items (c) and items (d), would follow in a further year (first half of 2004) and the final items at the end of a three year programme.

a) ***Cloud top height.*** The threshold value for cloud determination automatically generates a "cloud top height" or more accurately it provides the top tangent height at which a cloud is observed in MIPAS data (see point c) below). The cloud top height might more accurately be described as the "observed cloud top height".

b) ***Cloud index profiles.*** Cloud top height is a useful but somewhat simplistic product: a) the cloud may not be present at all altitudes below the top cloud height, e.g. broken or layered cloud; b) the cloud top height depends on the definition of a threshold value and changes in this parameter will lead to changes in cloud top height assigned; c) the definition of threshold value may depend on the purpose, e.g. one value might be specified for retrieval purposes, a larger value might be implemented to identify PSCs. Cloud index profiles should form a new product and a number of cloud indices could be defined (see point also d)).

c) ***Cloud location.*** The co-ordinates which specify cloud location are altitude, latitude and longitude. Nominally the co-ordinates assigned are those of the tangent height at which the cloud appears. However, since MIPAS is a spectrometer which observes the opacity of many spectral lines, it may be possible to use this information to better assign the cloud position along the line-of-sight (LOS) of the MIPAS instrument. This would allow a much more precise definition of location and would be an excellent product which would include a more accurate "Analysed cloud top height".

d) ***Cloud composition.*** It is quite clear that MIPAS observes different types of clouds, for example PSCs in the polar lower stratosphere and sub-visible cirrus in the lower troposphere. Recent research at Leicester has shown that there is very good potential to separate cloud types further based on: 1) the identification of specific spectral signatures, e.g. a PSC feature at 820 cm-1 which is believed to be NAT; 2) the observation of scattering effects (component of tropospheric radiation present) delivering information on particle mean size (work performed by IMK) and hence indicating particle type.

e) ***Aerosol extinction.*** If the composition study could be extended to differentiate aerosols (sulphate) from clouds, then it would be possible to retrieve vertical profiles of aerosol extinction (per km) from non-cloudy MIPAS data. Such data could possibly be derived from the continuum coefficients retrieved as part of the operational processing otherwise a dedicated retrieval would be required from specific microwindows.

f) ***Physical cloud parameters.*** Aerosol extinction is proportional to aerosol volume. Given a knowledge of cloud composition and given appropriate calibration curves for extinction vs. volume, it is possible to derive physical parameters of aerosol/clouds such as mean size and surface area. Furthermore, the observation of scattering effects affecting single spectra lines will provide additional constraints on possible particle sizes. These products are desirable for applications in climate studies and atmospheric chemistry.

11 ACKNOWLEDGEMENTS

This work has been funded through the ESA Expert Support Laboratory with support also from the European Commission through the MAPSCORE project EVK2-CT-2000-00072 and from the U.K. Natural Environment Research Council. The authors would like to acknowledge H. Nett, J. Langen and the ESL team for much helpful discussion and for data access.

12 REFERENCES

1. Carli, B., *et al*., Analysis of MIPAS measurements with the level 2 near real-time code, Proceedings of the ENVISAT Validation Workshop, Frascati, Italy, December, 2002
2. Mergenthaler, J. L., A. E. Roche, J. B. Kumer, and G. A. Ely, Cryogenic Limb Array Etalon Spectrometer observations of tropical cirrus *J. Geophys. Res*., 104, 22,183-22,194, 1999.
3. Massie, S.T. *et al*., Spectral signatures of polar stratospheric clouds and sulfate aerosols, *J. Atmos. Sci.*, *51*,3027,3044, 1994.
4. Taylor, F.W. *et al*., Properties of Northern Hemispheric Polar Stratospheric Clouds and Volcanic Aerosol in 1991/92 from UARS/ISAMS Satellite Measurements, *J.Atmos.Sci*, 51, 3019-3026, 1994.
5. Hervig, M.E., *et al*., Polar stratospheric clouds due to vapor enhancement: HALOE observations of the Antarctic vortex in 1993, *J. Geophys. Res.*, *102*, 28,185-28,193, 1997.
6. Offermann, D., K U. Grossmann, P. Barthol, P. Knieling, M. Riese, and R. Trant, The CRyogenic Infrared Spectrometers and Telescopes for the Atmosphere (CRISTA) experiment and middle atmosphere variability, *J. Geophys. Re*s., 104, 16,311-16,325, 1999.
7. Spang, R., G. Eidmann, M. Riese, P. Preusse, D. Offermann, L. Pfister, and P. H. Wang, CRISTA observations of cirrus clouds around the tropopause, *J. Geophys. Res*., 107(D23), 8174, doi:10/1029/2002JD000698 , 2002.
8. Dudhia, A., private communication, http://www.atm.ox.ac.uk/RFM/, 1997.
9. Remedios, J.J., Extreme Atmospheric Constituent Profiles for MIPAS, *Proceedings of the European symposium on atmospheric measurements from space*, ESTEC, Nordwijk, Netherlands, 20-22 January, Vol. 2, 779-783, 1999.
10. Riese, M., R. Spang, P. Preusse, M. Ern, M. Jarisch, D. Offermann, and K. U. Grossmann, Cryogenic Infrared Spectrometers and Telescopes for the Atmosphere (CRISTA) data processing and atmospheric temperature and trace gas retrieval, *J. Geophys. Res*., 104, 16349-16367, 1999.
11. Spang, R., M. Riese, and D. Offermann, CRISTA-2 observations of the south polar vortex in winter 1997: A new dataset for polar process studies, *Geophys, Res. Lett*., 28, 3159-3163, 2001a.
12. Spang, Reinhold; Remedios, John J. Observations of a distinctive infra-red spectral feature in the atmospheric spectra of polar stratospheric clouds measured by the CRISTA instrument, Geophys. Res. Lett.Vol. 30, No. 16, 1875, 10.1029/2003GL017231, 30 August 2003.